




REVIEW ARTICLE | JULY 25 2024

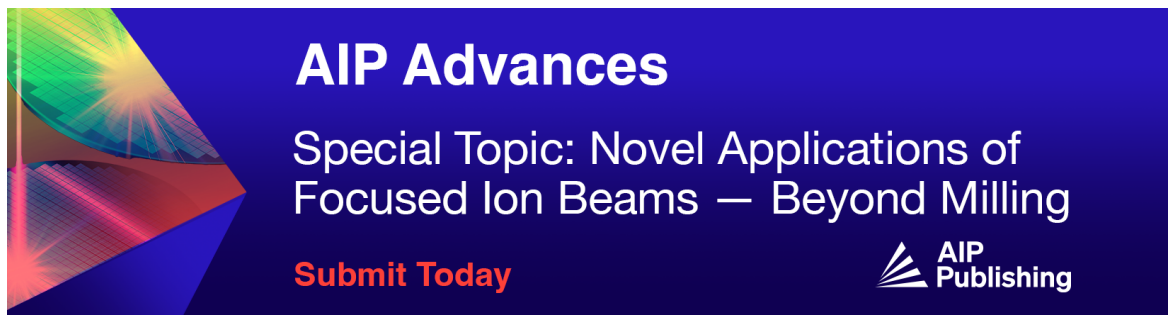
Exchange bias in Fe/FeF₂ and Fe/MnF₂ model systems

Tomasz Blachowicz ; Maciej Malczyk; Andrea Ehrmann  ; Martin Wortmann 




AIP Advances 14, 070703 (2024)

<https://doi.org/10.1063/5.0220475>



AIP Advances
Special Topic: Novel Applications of Focused Ion Beams — Beyond Milling
Submit Today



Exchange bias in Fe/FeF₂ and Fe/MnF₂ model systems

Cite as: AIP Advances 14, 070703 (2024); doi: 10.1063/5.0220475

Submitted: 25 May 2024 • Accepted: 10 July 2024 •

Published Online: 25 July 2024



View Online



Export Citation



CrossMark

Tomasz Blachowicz,¹  Maciej Malczyk,¹ Andrea Ehrmann,^{2,a)}  and Martin Wortmann³ 

AFFILIATIONS

¹Institute of Physics—Center for Science and Education, Silesian University of Technology, 44-100 Gliwice, Poland

²Institute for Technical Energy Systems (ITES), Faculty of Engineering and Mathematics, Bielefeld University of Applied Sciences and Arts, 33619 Bielefeld, Germany

³Bielefeld University, Faculty of Physics, 33615 Bielefeld, Germany

^{a)}Author to whom correspondence should be addressed: andrea.ehrmann@hsbi.de

ABSTRACT

The exchange bias (EB) is a unidirectional magnetic anisotropy that is found in structures containing exchange-coupled ferromagnetic/antiferromagnetic interfaces. The EB usually manifests as a horizontal shift of the hysteresis after cooling the system through the Néel temperature of the antiferromagnet in the presence of an external magnetic field. A vertical shift and an asymmetry of the magnetization loop are also possible. At present, the EB is often investigated for its effect on an application in magnetic devices in a variety of material systems and applications. The EB bilayer systems Fe/FeF₂ and Fe/MnF₂ represent an interesting case of structural similarities. In this paper, we show that differences between magnetic material orders and disorder contributions, found at the microscale, make them model systems for the occurrence of specific magneto-crystalline anisotropies and specific angular dependencies of the EB with significant implications for magneto-electronic applications.

© 2024 Author(s). All article content, except where otherwise noted, is licensed under a Creative Commons Attribution (CC BY) license (<https://creativecommons.org/licenses/by/4.0/>). <https://doi.org/10.1063/5.0220475>

I. INTRODUCTION

The unidirectional exchange bias (EB) anisotropy was discovered by Meiklejohn and Bean in Co/CoO core/shell particles.¹ The most prominent feature of the EB is a horizontal shift of the hysteresis loop after field cooling (FC) an exchange-coupled ferro-/antiferromagnetic (FM/AFM) layer system through the Néel temperature of the AFM, usually opposite to the cooling field direction.² In many cases, this horizontal shift is accompanied by a vertical shift and/or an asymmetry of the hysteresis loop.³

Besides the aforementioned experiments on FM/AFM core/shell particles, researchers have investigated EB systems in other shapes, often with a focus on thin film systems or nanostructured materials.^{4–6} The materials under investigation typically combine ferro- and antiferromagnetic layers but also include combinations with ferrimagnetic materials or even molecular materials that show an EB in a single phase. Among the most frequently investigated material combinations are Co/CoO and Co/Co₃O₄,^{7,8}

Fe/FeF₂,⁹ Fe/MnF₂,¹⁰ as well as more sophisticated systems, such as Fe/LaAlO₃¹¹ or Pr_{0.67}Sr_{0.33}MnO₃/SrTiO₃.¹²

Today, these relatively old results are still in use as the basis for the development of new functionalities and properties in new material combinations. Recently, the research on EB systems partly focused on amorphous thin films in which structural magnetic disorder dominates, as opposed to epitaxial order. In recent studies by Masood *et al.*, spin glass-like behavior in Fe–B–Nb amorphous thin films was recognized as influenced by structural anomalies and confirmed experimentally by magneto-thermogravimetry.¹³ The level of structural irregularities is enhanced in amorphous materials. Kedia *et al.* showed that an increase in the grain diameter of the antiferromagnetic layer led to a positive EB in Co₂FeAl/Ir₇Mn₉₃,¹⁴ similar to the positive EB found in some Fe/FeF₂ bilayer systems. It should be mentioned that the authors found positive EB only at room temperature, while after field-cooling to 15 K, this system revealed negative EB. A similar bilayer system, CoFeB/IrMn, was numerically studied to confirm strain-induced 1.5 times enhancement of

the EB.^{15,16} This study is a great example of the connection between factors influencing a system on different scales, such as the change of lattice parameters due to mechanical stress, which also induces a fourfold anisotropy and modifies the spin-orbit coupling in the material.

IrMn-based devices found applications in giant magnetoresistance (GMR) sensor applications, making such EB systems attractive for potential applications. NiFe/IrMn was recently studied by Kedia *et al.*, where different structural factors, such as atomic roughness and crystalline grain sizes, were investigated.¹⁷ For polycrystalline samples, based on Heusler alloys that are of great importance for ultra-high-density storage devices, Tian *et al.* studied the influence of the martensitic phase in $\text{Ni}_{50}\text{Mn}_{38}\text{Sb}_{12-x}\text{Ga}_x$ for $x < 13$,¹⁸ where they identified the coexistence of ferromagnetic and antiferromagnetic phases, with the EB being tuned by composition and temperature. Importantly, they identified a temperature-controlled competition mechanism between the ferromagnetic orthorhombic martensite phase and the antiferromagnetic tetragonal austenite phase.

The underlying effects related to structural and thermodynamic factors, revealed in these recent studies, will be analyzed in detail in Secs. II–V. This article gives an overview of the specific properties of Fe/FeF₂ and Fe/MnF₂ bilayers, explains the unusual angular dependence of the EB in Fe/MnF₂ thin film systems, and compares previous results in both systems with other material combinations that were investigated recently and can be better understood on the basis of physical effects revealed originally in Fe/FeF₂ and Fe/MnF₂ EB systems. It should be mentioned that Fe/FeF₂ and Fe/MnF₂ behave in many ways different from the widely studied EB system Co/CoO, as will be described in Secs. II–V.

Understanding these model systems and similar systems, such as EB systems with IrMn as AFM, will support the development of novel spintronics elements and quaternary magnetic storage devices.

II. MAGNETIC PROPERTIES AND SPIN STRUCTURE

While the Curie temperature of iron is 1043 K¹⁹ and, thus, far above common temperatures reached in spintronics applications, both Néel temperatures of the AFMs are far below room temperature (RT). For FeF₂, the Néel temperature is often assumed as $T_N = 78$ K,²⁰ but much smaller and even slightly larger values can be found depending on the layer thickness and strain.^{21,22} A similar value of 67 K is reported as the Néel temperature of Fe/MnF₂.^{23,24} It should be mentioned that the blocking temperature, i.e., the temperature above which the exchange bias vanishes, can be significantly lower than the Néel temperature but also similar to the Néel temperature, e.g., in systems with polycrystalline CoO as AFM and in many cases in systems containing FeF₂ or MnF₂ as AFM.²

In Fe/MnF₂ and Fe/FeF₂ thin film systems, the spin structure has been reported by some researchers. Sahoo prepared Al(3 nm)/Fe(8 nm)/MnF₂(52 nm)/ZnF₂(16 nm)/MgO(001) samples by electron beam evaporation, where the ZnF₂ buffer layer was used to relax the lattice mismatch between MnF₂ and MgO(100).²⁵ The MnF₂ layer grew quasi-epitaxially in (110) orientation with a pseudo-twinned lattice, i.e., with the easy axes oriented $\pm 45^\circ$ to the MgO [100] directions, which was also reported by other researchers using similar sample preparation procedures.^{26–28} Sahoo found the Fe spins to always lie in the sample plane and to rotate in-plane away from the directions of the remanent magnetization toward the next AFM easy axes during zero field cooling (ZFC), while no such rotation of the Fe spins was observed between the Néel temperature and RT. The spin rotation was reduced during FC due to the competition between exchange coupling with Mn spins oriented along the easy axes of MnF₂ and orientation along the external magnetic field.²⁵ The reorientation of the FM spins in Fe/FeF₂ and Fe/MnF₂ was theoretically investigated by Silva *et al.* who showed that this reorientation occurred in uniaxial FM films only for a sufficiently strong interface field, while it always occurred in fourfold FM films.²⁹

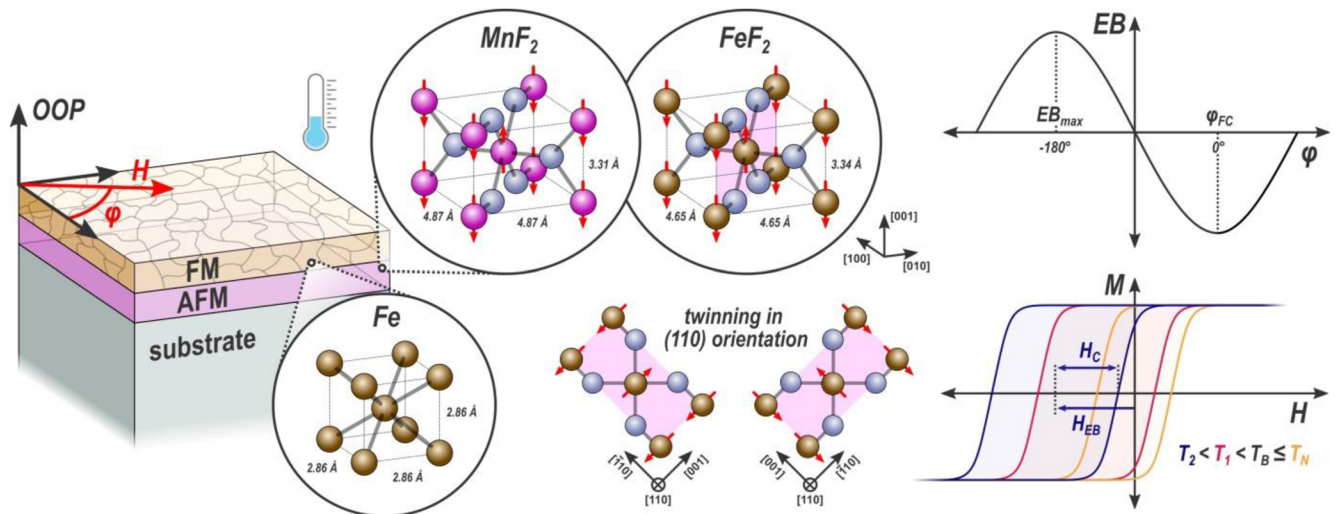


FIG. 1. Spin structures of Fe, MnF₂, and FeF₂ in a typical thin-film system (left), typical exchange bias (top right), and typical temperature dependence of the exchange bias (EB) (bottom right side).

Sahoo also investigated the spin structure of Fe/FeF₂ films prepared as Al(3 nm)/Fe(8 nm)/FeF₂(45 nm)/MgO(100).²⁵ The FeF₂ layer was again found to be (110) pseudo-twinned with the easy axis being oriented $\pm 45^\circ$ to the MgO[100] directions, as also reported in other studies.^{30,31} The Fe spins always lie in the sample plane, as in the above-described Fe/MnF₂ samples.²⁵ The in-plane spin structure, however, differed: In Fe/FeF₂ films, the FM spins were oriented near the AFM easy axes (i.e., $\pm 45^\circ$ to the MgO[100] directions and also $\pm 45^\circ$ to the external magnetic field) even at room temperature. ZFC from 200 to 90 K led to a continuous rotation away from the AFM easy axes, which was attributed to the high-temperature magnetic anisotropy of FeF₂, while further cooling below the Néel temperature rotated the FM spins back to the AFM easy axis directions.²⁵ Kiwi *et al.* found a canted spin configuration in the AFM interface frozen in a metastable state near the Néel temperature, leading to the EB energy being stored in a spring-like magnet or incomplete domain wall.³²

An overview of spin structures of the materials under investigation here is shown in Fig. 1 (left part), combined with a typical pseudo-twinned (110) AFM layer, a typical cosine-shaped angular dependence of the EB (top right part), as well as common hysteresis loops for different temperatures below and at the Néel temperature (bottom right side).

It should be mentioned that other thin-film orientations can be achieved by using different substrates and/or buffer layers. However, these detailed investigations of the often chosen (110) pseudo-twinned AFM layer already show that a different temperature dependence and potentially different angular dependence of the EB in Fe/FeF₂ and Fe/MnF₂ thin-film systems can be expected.

This article is structured as follows: Sec. III gives an overview of the temperature dependence of Fe/FeF₂ and Fe/MnF₂ EB systems. The cooling field dependence is discussed in Sec. IV. The angular dependence of the EB in these systems for varying cooling fields and measurement angles is examined in Sec. V; finally, Sec. VI gives a conclusion and outlook toward potential new magneto-electronics and spintronics devices based on such EB systems.

III. TEMPERATURE DEPENDENCIES

While some studies compare Fe/FeF₂ and Fe/MnF₂ above and below their respective Néel temperatures, only a few researchers report more detailed measurements of the temperature dependence of the EB and coercive fields. In this section, we discuss such studies.

A. Fe/FeF₂

Fitzsimmons *et al.* investigated the temperature-dependent properties of Fe/FeF₂ thin-film samples with untwinned (110) single crystalline, twinned (110) single crystalline, or (110) polycrystalline FeF₂ layers, while Fe was polycrystalline in all samples.³³ They only found an asymmetric magnetization reversal for the twinned (110) AFM measured at a sample orientation of $\pm 45^\circ$ to the AFM easy axes, while the magnetization reversal was symmetric for the same sample measured along 0° or 90° to the AFM easy axes as well as for both other samples.^{33,34} The temperature dependence of the coercive field showed a peak near the Néel temperature for the untwinned sample measured along the hard or the easy axis,³³ which is well-known from Co/CoO(110) where the 90° coupling also induces a

peak in the coercivity near the Néel temperature due to an exchange of hard and easy axes.⁷ This 90° rotation of the ferromagnetic easy axis due to the AFM ordering was also reported by Moran *et al.* who found a peak in the coercivity only along the FeF₂[100] direction of the untwinned AFM, as shown in Fig. 2.³⁵

Nogués *et al.* compared FeF₂ thin-film samples to bulk single crystals in different orientations, on which polycrystalline Fe films were grown with (110) and (100) preferred orientations.³¹ They found similar blocking temperatures near the Néel temperature in all cases, but strongly varying EB values at low temperatures between ~ -180 Oe for thin-film FeF₂(110)(~ 90 nm)/Fe(~ 13 nm)/Ag(~ 9 nm) samples on a MgO(100) substrate and even positive values up to $\sim +60$ Oe for Fe(~ 20 nm)/Ag(~ 20 nm) grown on a (110) FeF₂ polished-annealed substrate, field-cooled along the AFM easy axis.³¹

For a polycrystalline Fe film (~ 13 nm) with preferred (110) and (100) orientations grown on top of twinned (110) FeF₂ layers (~ 90 nm), Nogués *et al.* also found the blocking temperature to be near the Néel temperature.³⁰ Depending on the cooling field, they found an EB of ~ -210 Oe (for FC in 2 kOe) or $\sim +240$ Oe (for FC in 70 kOe) at low temperatures, followed by a plateau up to ~ 40 K for the negative EB and even a maximum at ~ 40 K for the positive EB.³⁰ A similar temperature dependence was reported by Widuch *et al.* for a single-crystal FM (2.5 nm Fe)/polycrystalline AFM (50 nm FeF₂), where the EB starts at low temperatures around -210 Oe, stays approximately constant up to around 30 K and then decreases rapidly until the blocking temperature that was again quite near the Néel temperature.³⁶ The coercivity, on the other hand, decreases constantly with increasing temperature with $\sim 1/T$. The depicted hysteresis loops measured at 17 and 85 K are mostly symmetric.³⁶ Using Kerr microscopy, the authors found domain patterns typical

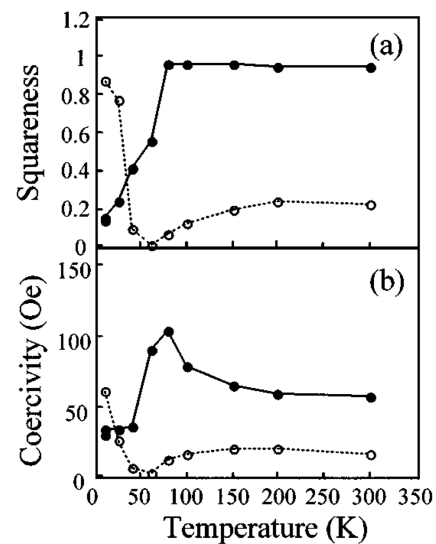


FIG. 2. Squaresness (a) and coercivity (b) for an Ag(20 nm)/Fe(20 nm)/FeF₂(110) sample. Field applied in-plane parallel to the FeF₂[001] direction (filled circles) and FeF₂[1, -1, 0] direction (open circles). Here, squaresness is defined as remanent magnetization divided by saturation magnetization. Reproduced from Moran *et al.*, Perpendicular coupling at Fe-FeF₂ interfaces. Appl. Phys. Lett. **72**, 617 (1998) with the permission of AIP Publishing LLC.

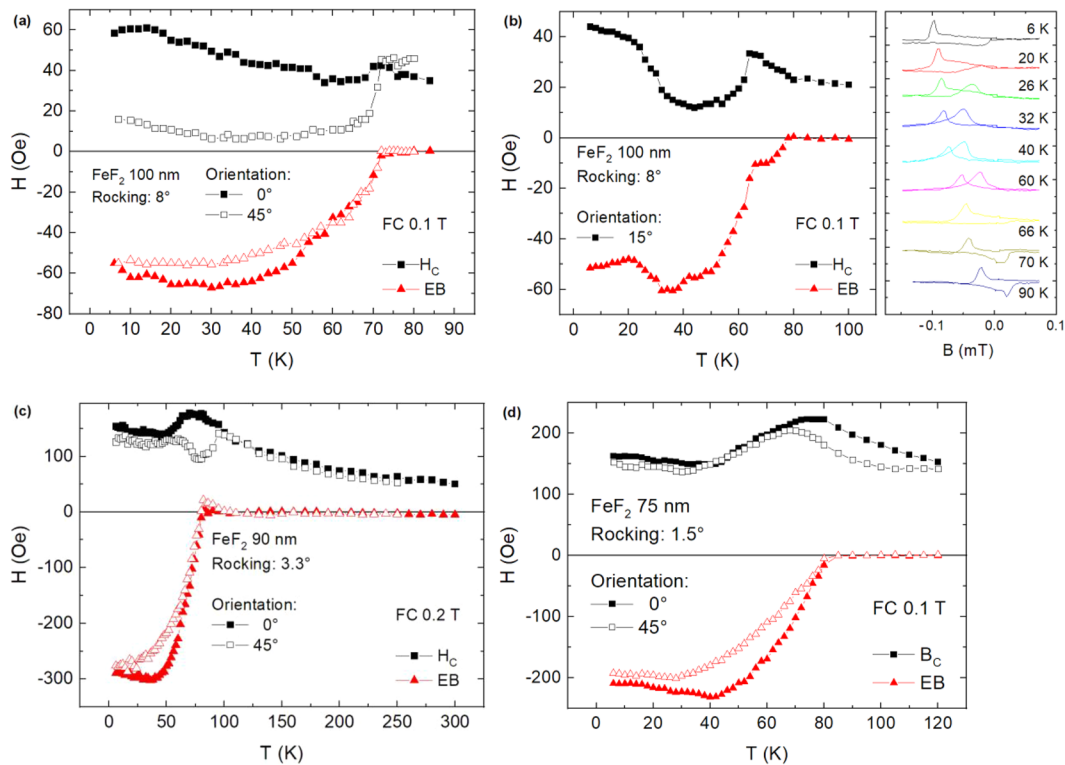


FIG. 3. Temperature-dependent exchange bias (EB) and coercive fields (H_c) for different thin film samples: (a) and (b) FeF_2 100 nm, rocking curve width (defining the roughness) 8° , Fe with (110) texture; (c) FeF_2 90 nm, rocking curve width 3.3° , Fe with (100) texture; and (d) FeF_2 75 nm, rocking curve width 1.5° , Fe with (100) texture. Reprinted from Tillmanns, Magnetisierungsumkehr und -dynamik in Exchange-Bias-Systemen, Dissertation thesis, RWTH Aachen, Germany, 2005. Copyright 2005, published open access; modified.

for cubic anisotropy at room temperature, while patch-like magnetic domains formed below the blocking temperature.³⁶ This is similar to the results of Monte-Carlo simulations of Co/CoO EB systems with diluted antiferromagnets.³⁷

In a Monte Carlo simulation of Fe/Fe₂(100) bilayers with an uncompensated interface, Li *et al.* found a slight variation of the temperature dependences of EB and coercivity with the AFM/FM mixing at the interface, where the blocking temperature varied with the surface roughness.³⁸ A small maximum of the coercivity near the blocking temperature was visible. A small range of the interface mixing parameter led to positive EB, of which the temperature dependence was not depicted.³⁸

For thin-film samples with twinned FeF₂(110) and polycrystalline Fe layer with preferred (110) and (100) orientations, different AFM thicknesses and corresponding interface roughnesses resulted in different orientations of the Fe layer, which showed either mostly twofold or mostly fourfold anisotropies at room temperature.³⁹ Figure 3 depicts exemplary temperature-dependent measurements for different sample orientations.³⁹ Depending on the interface roughness (larger rocking curve widths indicate rougher interfaces), the absolute values of coercivity and EB differ strongly. Smoother interfaces resulted in larger coercivity [Fig. 3(d)], while the largest EB is found for an intermediate roughness [Fig. 3(c)]. Other studies

on FeF₂, but also on other systems, such as Co/CoO, showed higher or lower sensitivity to interface roughness, with the EB either increasing or decreasing with higher interface roughness.² The coercivity at low temperature, measured along 0° and 45° sample orientation, differs strongest for the only sample in which Fe grew with (110) preferred orientation [Fig. 3(a)]. This may be attributed to the angle-dependent asymmetry of the magnetization reversal, as shown by the transverse magnetization components [inset in Fig. 3(b)] at 15° sample orientation. However, most of the aforementioned temperature dependencies of EB and coercive field can be found here, too—a blocking temperature near the Néel temperature and a slight increase in the EB near 40 K for measurements along the MgO[001] orientation (here 0° orientation). Interestingly, both samples with fourfold Fe texture [Figs. 3(c) and 3(d)] even show a broad range of increased coercivity around the Néel temperature, which was usually found in samples with untwinned FeF₂(110) layers.

B. Fe/MnF₂

For samples of MgO(001)/ZnF₂(25 nm)/MnF₂(50 nm)/Fe(11 nm)/Al(3 nm), Fitzsimmons *et al.* reported a constantly decreasing EB that vanished near the Néel temperature.²⁷ Here, the ZnF₂ buffer layer improved the epitaxial growth of the subsequent

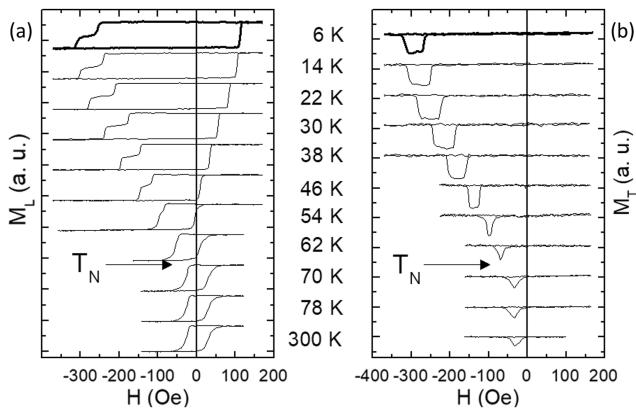


FIG. 4. Temperature dependence of the (a) longitudinal and (b) transverse magnetization components of $\text{MnF}_2(110 \text{ twinned})/\text{Fe}[\text{polycrystalline with } (110) \text{ and } (100) \text{ preferred orientations}]$. Reprinted from Tillmanns, *Magnetisierungsumkehr und -dynamik in Exchange-Bias-Systemen*, Dissertation thesis, RWTH Aachen, Germany, 2005. Copyright 2005, published open access; modified.

MnF_2 layer that was shown to grow in twinned (110) orientation, with the easy axes oriented $\pm 45^\circ$ to the $\text{MgO}[100]$ directions, as is often found in Fe/FeF_2 samples, while FC was performed along 0° , as in most cases. The deposition temperature of the AFM was varied to obtain interface roughnesses of 1.9 and 0.5 nm, respectively, where the sample with a smoother interface showed a slightly larger EB at intermediate temperatures.²⁷

An almost constant EB of ~ -80 Oe up to a temperature of 50 K was reported by Macedo *et al.* before the EB was significantly reduced and vanished around the Néel temperature.⁴⁰ For their experiments, samples with 70 nm Fe on top of 52 nm $\text{MnF}_2(110)$ on a $\text{ZnF}_2(110)$ buffer were used, where the MnF_2 film was again twinned, and the Fe layer grew polycrystalline. Similarly, Sahoo

found in the afore-described samples a constant reduction in coercivity with increasing temperature, while the EB was approximately constant up to 50 K and then rapidly decreased toward the Néel temperature.²⁵

In samples with a wedge-shaped Fe layer [polycrystalline with (110) texture, thickness 1.6–16 nm] on top of a twinned 65 nm $\text{MnF}_2(110)$ film, Leighton *et al.* found a clear dependence of the coercivity on the Fe layer thickness, with thinner FM layers resulting in much higher coercivities at low temperatures.⁴¹ For the samples with thinner Fe layers, they found the expected decrease in the coercivity with increasing temperature, while thicker Fe layers resulted in approximately constant coercive fields up to 75 K or even a slight increase of the coercivity near the Néel temperature. In addition, they showed that for a Fe thickness of 12 nm, a sample with an AFM thickness of 220 nm led to a steady decrease in coercivity with increasing temperature, while a reduction of the AFM thickness to 21 nm resulted in a small peak of the coercivity at the Néel temperature. At 10 K, the EB increased from ~ -35 to -300 Oe with decreasing AFM thickness; a temperature dependence of the EB was not reported.⁴¹

In a sample $\text{MgO}(100)/\text{ZnF}_2(110)/\text{MnF}_2(110)/\text{Fe}(\text{polycrystalline})/\text{Al}(\text{cap layer})$ with thicknesses 25 nm/50 nm/12 nm/5 nm and a twinned AFM, Leighton *et al.* found the EB decreasing from ~ -50 Oe at 5 K to zero at the Néel temperature.⁴² They also showed a clear asymmetry of the hysteresis loop with a broad step on the left side (after field cooling in a positive field direction), which was reduced similarly to the EB with increasing temperature. The authors attributed this step in the loop to an intermediate metastable state of the magnetization, oriented 90° to the original magnetization direction, while magnetization reversal on the right side was assumed to occur by domain wall nucleation and propagation.⁴²

A more detailed examination of the step in the longitudinal hysteresis loop and the corresponding peak in the transverse magnetization component can be found in Ref. 39. As Fig. 4 shows, both the step and the peak are broadest at low temperatures, measured for a sample $\text{Al}(3 \text{ nm})/\text{Fe}(12 \text{ nm})/\text{MnF}_2(65 \text{ nm})/\text{ZnF}_2(25 \text{ nm})/$

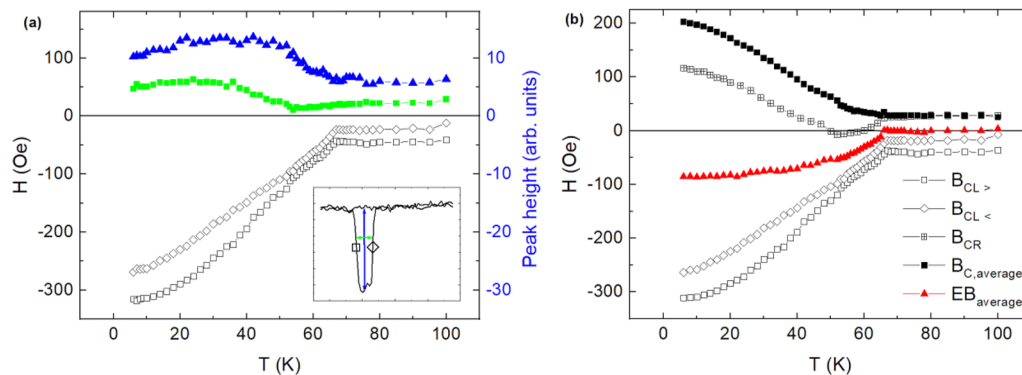


FIG. 5. (a) Temperature dependence of the position (black open symbols), width (green squares), and height (blue triangles) of the transverse peaks of $\text{MnF}_2(110 \text{ twinned})/\text{Fe}[\text{polycrystalline with preferred } (110) \text{ and } (100) \text{ orientation}]$ sample; the inset describes the measured values. (b) Temperature dependence of the inner and outer left coercivity $B_{CL>}$ and $B_{CL<}$, the right coercivity B_{CR} , and the herewith calculated average coercivity $B_{C,average}$ and exchange bias $EB_{average}$. Reprinted from Tillmanns, *Magnetisierungsumkehr und -dynamik in Exchange-Bias-Systemen*, Dissertation thesis, RWTH Aachen, Germany, 2005. Copyright 2005, published open access; modified.

MgO(001) with a twinned MnF₂(110) layer, with the MnF₂(110) twins being oriented along $\pm 45^\circ$ to the MgO[100] directions. The rocking curve width for the sample surface is 2.0° , indicating a low roughness. The Fe layer had preferred (110) and (100) orientation.³⁹ The asymmetric peak above the Néel temperature [Fig. 4(b)] was attributed to a slight mismatch between the sample's crystallographic axes and the external magnetic field.¹⁰

Similar to Ref. 42, the temperature-dependent width of the peak and its position and height were evaluated [Fig. 5(a)], showing a constant decrease in the peak position with temperature, while the peak height and width stayed approximately constant below ~ 50 and 30 K, respectively.³⁹ The corresponding longitudinal switching fields on the left side (similar to the peak positions) and coercivity on the right side of the longitudinal hysteresis loops are depicted in Fig. 5(b) and show an EB that is mostly constant in a broad temperature range before it vanishes at the Néel temperature.³⁹ For similar samples with rougher surfaces and mostly (100) textured Fe layers, the measured EB values were smaller but showed a qualitatively similar behavior.³⁹

IV. COOLING FIELD DEPENDENCE OF THE EXCHANGE BIAS

As mentioned before, the cooling field may influence the value of the EB shift and in some systems even change its sign. This section reports about the cooling field dependence of Fe/FeF₂ and Fe/MnF₂, which is often very different compared with other systems, such as Co/CoO.²

Some researchers report a positive EB in Fe/FeF₂, i.e., in the direction of the cooling field, for large enough cooling fields. In twinned FeF₂(110) and polycrystalline Fe with preferred (110) and (100) directions, Nogués *et al.* reported a large EB of -500 Oe at 10 K, where the FeF₂ was grown at 200°C after cooling in a small field. However, samples with FeF₂ layers grown at 250 or 300°C started with an EB of -200 Oe at 10 K for small cooling fields and switched to positive EB at cooling fields of 10 kOe, and even reached large positive EB values of $+150$ – 200 Oe for large cooling fields of 70 kOe.³⁰ The positive EB was attributed to the competition between FM–AFM exchange interaction and an external field–AFM surface magnetic coupling interaction. In addition, they found a strong dependence of the coercivity on the cooling field only for a sample orientation of 0° , i.e., $\pm 45^\circ$ orientation of the FeF₂ twin's easy axes, while field cooling and measuring along the twin's easy axes resulted in only a small variation of the coercivity with the cooling field.³⁰

A positive EB was also reported by Nogués *et al.* for different Fe/FeF₂ and Fe/MnF₂ samples.⁴³ They reported the dependence of the EB on the growth temperature of the AFM for both material systems. The authors found the sign change of the EB with increasing cooling field to be correlated with a sign change of the vertical shift of the hysteresis loops for Fe/FeF₂ where the AFM was grown at 300°C as well as for Fe/MnF₂ with the AFM grown at 275°C . They stated that the interface coupling was responsible for the EB found for large cooling fields, while small cooling fields resulted in a more complex correlation between EB and coupling sign.⁴³

Similar to Ref. 30, Kiwi *et al.* discussed the possibility of a positive exchange bias for EB systems including AFMs with strong anisotropy, especially Fe/MnF₂ and Fe/FeF₂, based on the interface coupling.⁴⁴ Interestingly, they calculated positive EB to occur

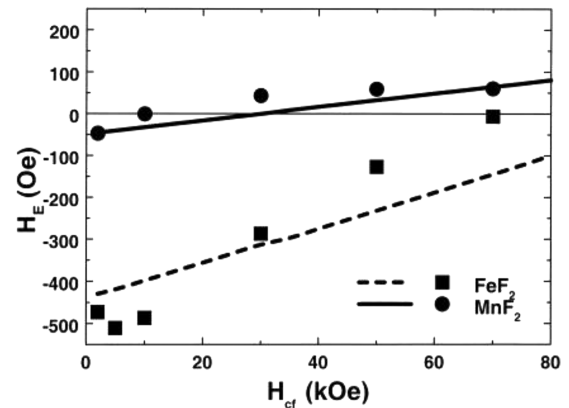


FIG. 6. H_E vs cooling field H_{cf} for Fe/FeF₂ and Fe/MnF₂. The lines are theoretical results and the circles and squares correspond to the experiments in Ref. 43. Reproduced with permission from Kiwi *et al.*, Positive exchange bias model: Fe/FeF₂ and Fe/MnF₂ bilayers, Solid State Commun. **116**, 315 (2000). Copyright 2000, Elsevier.

in Fe/MnF₂ (Fig. 6), while this effect was experimentally more often reported for Fe/FeF₂.

It should be mentioned that field cooling and measuring was in most cases performed along an easy axis of the AFM, i.e., along $\pm 45^\circ$ with respect to the (110) twins in case of a twinned AFM. The dependence of the EB on the cooling field and measuring orientation will be discussed in Sec. V.

V. ANGULAR DEPENDENCE OF THE EXCHANGE BIAS

In this section, we differentiate between measurements where the sample was cooled along a specific (typically easy) crystallographic axis and subsequently rotated at low temperatures, and on the other hand, investigations where the sample was field cooled at varying cooling field angles. Studies in which the cooling field angle is unclear are not discussed.

A. Angular dependence of EB and coercivity in general EB systems

First, it should be mentioned that the uniaxial EB anisotropy is usually assumed to have a cosine angular dependence, with the maximum EB parallel and antiparallel to the cooling field direction, as shown in the literature for diverse EB systems, such as FeMn/(FeNi/FeMn)_n multilayers, IrMn/Co, IrMn/FeNi, Fe_xZn_{1-x}F₂/Co, or Fe/MnPd.^{45–49} On the other hand, some researchers mentioned measurements of an angular-dependent EB or coercivity that could not fully be explained by the common Meiklejohn and Bean model⁵⁰ or Stoner–Wohlfarth model.⁵¹

Radu *et al.* used a modified Meiklejohn and Bean model to explain measurements on CoFe/IrMn samples with twofold anisotropy. They assumed an additional spin disorder at the FM/AFM interface, i.e., an interlayer with zero anisotropy next to the FM and increasing anisotropy toward the main part of the AFM, until the AFM anisotropy constants are reached.⁵⁰ Nevertheless, the cosine angular dependence remained unchanged.⁵²

Geshev *et al.* mentioned that a distribution of AFM easy axes could modify the angular dependence of EB and coercivity so that peaks were softened.⁵³

For NiFe(111)/FeMn(111)/CoFeB(amorphous), Singh and Chaudhary reported a clear cosine dependence of the EB on the in-plane angle, but a deviation between the uniaxial and unidirectional easy axes, which they attributed to the interface roughness.⁵⁴ An apparently more complex angular dependence in MgO/NiO/Co samples was reported by Dubourg *et al.*⁵⁵ Similarly, complex angular dependencies of the EB can be found in simulations with four-fold, uniaxial, and unidirectional anisotropy using the standard mathematical descriptions.⁵⁶ Dubourg *et al.* also showed fits with a Stoner–Wohlfarth coherent rotation model including these three anisotropies, which approximated the experimental values relatively well.⁵⁵ Liedke *et al.* showed the effect of non-collinear unidirectional and uniaxial anisotropy in rippled Ni₈₁Fe₁₉/Fe₅₀Mn₅₀, without changing the cosine term itself.⁵⁷ In Co/CoO core-shell nanowire, Gandha *et al.* showed a deviation from the usual cosine-like angular dependence of the EB that they attributed to a misalignment of the FM and AFM spins at the core-shell interface.⁵⁸

A novel mathematical approach was mentioned by Radu *et al.* who simulated epitaxially grown FeNi(111)/CoO(111) bilayers.⁵⁹

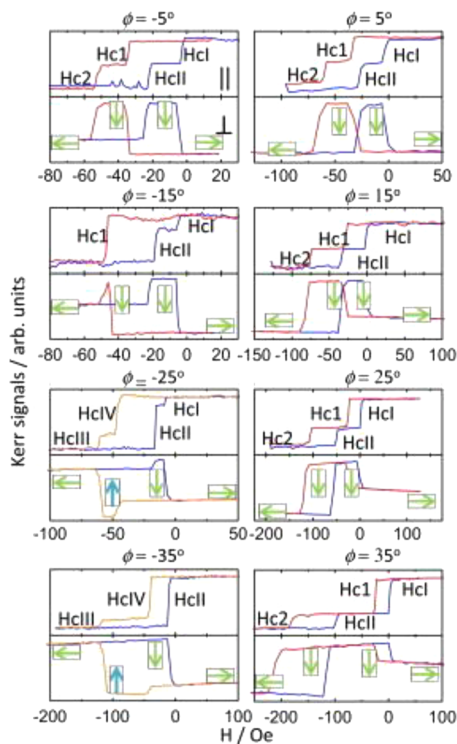


FIG. 7. Longitudinal (||) and transverse (⊥) MOKE loops measured at selective field angles for the non-collinear anisotropy configuration ($\alpha_{FC} = -21^\circ$ with respect to an Fe easy axis). The orientation of Fe spins in the switching processes is represented by the arrows enclosed in a box. Reproduced with permission from Zhang and Krishnan, Domain wall nucleation in epitaxial exchange-biased Fe/IrMn bilayers with highly misaligned anisotropies, *J. Magn. Magn. Mater.* **324**, 3129 (2012). Copyright 2012, Elsevier.

While they did not show the angular dependence of the EB, they measured the angle dependent spin flip and non-spin flip Bragg peak integrated intensities in x-ray scattering and found a clear sixfold anisotropy, as expected, but with sharp peaks, which they attributed to the AFM spins being aligned with the sixfold crystallographic axes.⁵⁹ For Fe(001)/IrMn(001), Zhang and Krishnan showed interesting longitudinal magnetization loops with one or two steps as well as corresponding transverse magnetization loops with partly very broad, nearly rectangular peaks, similar to those depicted for Fe/MnF₂ in Fig. 4.⁶⁰ Parts of their measurements are shown in Fig. 7.⁶⁰ These measurements were performed for a field cooling angle deviating 21° from the next Fe easy axis. Similar to the aforementioned study, here the authors defined the EB to be oriented in two orthogonal cubic easy axes, resulting in an effective field superimposed on the Fe easy axes. In this way, they could well explain the magnetization reversal directions, i.e., the sign of the transverse magnetization peaks, as well as the switching fields along the whole angular range.⁶⁰ A very similar idea was described by Hajiri *et al.* for CFN(001)/MnN(100) bilayers, which also showed broad, nearly rectangular transverse peaks if the system was measured along other than the field cooling direction.⁶¹ This idea will be discussed for Fe/MnF₂ in Secs. V D and V E.

B. Fe/FeF₂–FC at easy axis

For Fe/FeF₂ thin films with twinned FeF₂(110) and polycrystalline Fe, Miltényi *et al.* found a clear fourfold anisotropy at room temperature with easy axes along $n \cdot 90^\circ$ with respect to the [001] directions.⁶² After field cooling along a hard axis (45°), spin wave frequencies were measured at 50 K and fitted with a cosine function for the EB, leading to a difference of $\sim 25\%$ between the EB calculated from the spin wave frequencies and from static hysteresis loops, which the authors attributed to potential higher order terms for the unidirectional anisotropy.⁶²

The asymmetry of the transverse peak reversal around the easy axis was shown in FeF₂(110 twinned)/Fe [polycrystalline with (110)

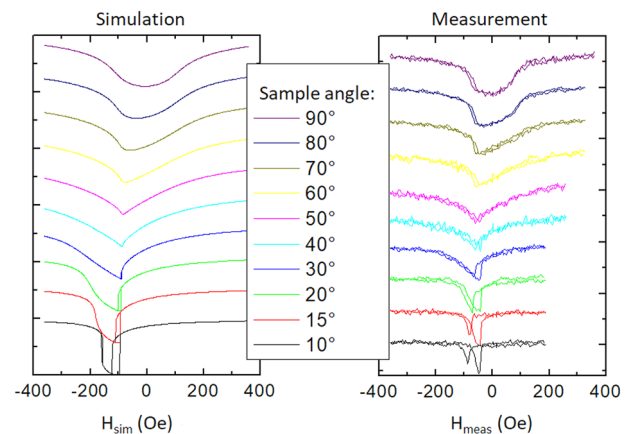


FIG. 8. Transverse magnetization components: simulated (left) and measured (right) after field cooling along the AFM easy axis at 0° to $T = 20$ K. Reprinted from Tillmanns, Magnetisierungsumkehr und -dynamik in Exchange-Bias-Systemen, Dissertation thesis, RWTH Aachen, Germany, 2005. Copyright 2005, published open access; modified.

texture] after field cooling along the easy axis, causing variation of the EB in this angular range, which agreed with simulations by a simple macrospin model assuming a cosine function for the EB.⁹ Measurements of the transverse magnetization component compared with a macrospin simulation with a cosine-like EB can be found in Ref. 39 for a broader angular range up to 90° from the cooling field direction, as depicted in Fig. 8. While the shapes of the transverse magnetization loops are modeled relatively well with the macrospin model, i.e., under the assumption that magnetization reversal occurs completely by coherent rotation, the EB values are overestimated. It may be speculated that the rotation of the magnetization—which is apparent due to the large transverse peaks—is not fully coherent, but contains a fanning of the FM spins, as it can be assumed in a not perfectly homogeneous sample. However, these simulations are not sufficient to state the necessity of a non-cosine-shaped EB term.

C. Fe/FeF₂—Varying cooling field angles

In this section, different cooling field directions in Fe/FeF₂ are discussed. Olamit *et al.* examined different EB systems, among others a fully polycrystalline Fe/FeF₂ thin-film sample, for which they reported that field cooling at varying in-plane angles resulted in a constant EB measured at each cooling field angle, while always measuring at 0° led to a cosine-shaped exchange bias.⁶³ This is not unexpected for a system with polycrystalline AFM, i.e., with arbitrarily distributed AFM easy axes.

Oppositely, in a twinned FeF₂(110) film and polycrystalline Fe layer with (110) texture, the angles of the sign change of the transverse peaks were not identical with the cooling field directions but varied around them with a fourfold plus uniaxial symmetry, as it is expected from a fourfold AFM coupled to an FM with uniaxial anisotropy (Fig. 9).⁹ This behavior could be fitted well with a cosine-shaped EB term in a macrospin model; however, the authors

emphasized that the reproduction of the measured phase diagram was only possible if they assumed that the direction of the EB was not identical with the cooling field direction but was varied by the strong fourfold anisotropy of the AFM.⁹ More precisely, the EB direction was assumed to be identical with the cooling field direction only along hard and easy fourfold axes, while it was slightly moved toward the nearest easy axis for any other cooling field angle. The calculated shift of the EB direction with respect to the cooling field direction is depicted in Fig. 9(a) as a blue line.⁹ A completely different phase diagram was found in another Fe/FeF₂ system with (100) textured FM and twinned (110) AFM [Fig. 9(b)].³⁹ Here, the angles of the sign change for the left and the right peak are approximately identical. For field cooling between 0° (easy axis) and 40°, the peak signs always change around 0°, while they change their sign around 90° for a cooling field angle of 50°–90°. Only field cooling very near to the hard axis (45°) leads to changing the signs of the peaks at intermediate angles.³⁹ Apparently, the crystallographic orientation of the ferromagnet significantly changes the cooling field angle dependence of the angles where the transverse peaks change their sign: Smooth variations of the peak sign angles as well as the EB direction around the cooling field direction can be found for a (110) textured FM with unidirectional anisotropy; an abrupt switch of the peak sign change angles—and potentially also the EB direction, which was not sufficiently simulated in Ref. 39—is found in the case of a fourfold (100) textured FM.

D. Fe/MnF₂—FC at easy axis

As discussed in Secs. II–IV, the longitudinal and transverse magnetization curves of Fe/MnF₂ and Fe/FeF₂ differ significantly and can, thus, also be expected to differ in terms of anisotropy energies. Arenholz and Liu showed phase diagrams for MnF₂(110 twinned)/polycrystalline Fe thin-film sample fields cooled along the easy AFM axis (0°).⁶⁴ They found that the measurement in

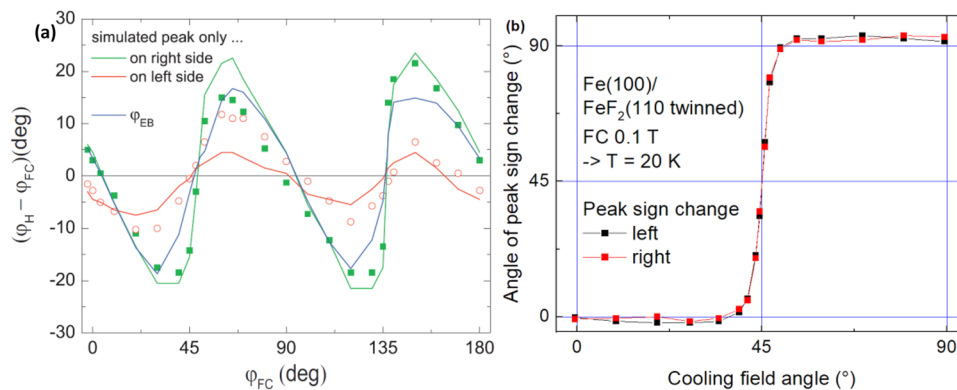


FIG. 9. (a) Measured phase lines (full green squares and open red circles, averaged for better statistics over the two 180° intervals), EB angle ϕ_{EB} (blue line), and resulting simulated phase lines (green and red lines). Above the upper phase line, both transverse peaks are negative, while below the lower phase line, both transverse peaks are positive. One positive and one negative peak can be found between the field lines. AFM easy axes are located near 0° modulo 90°. Reproduced with permission from Tillmanns *et al.*, Angular dependence and origin of asymmetric magnetization reversal in exchange-biased Fe/FeF₂(110), Phys. Rev. B **78**, 012401 (2008). Copyright 2008, American Physical Society. (b) Measured phase diagram of the peak sign change for a thin-film sample with Fe with (100) texture and twinned FeF₂(110). Reprinted from Tillmanns, Magnetisierungsumkehr und -dynamik in Exchange-Bias-Systemen, Dissertation thesis, RWTH Aachen, Germany, 2005. Copyright 2005, published open access; modified.

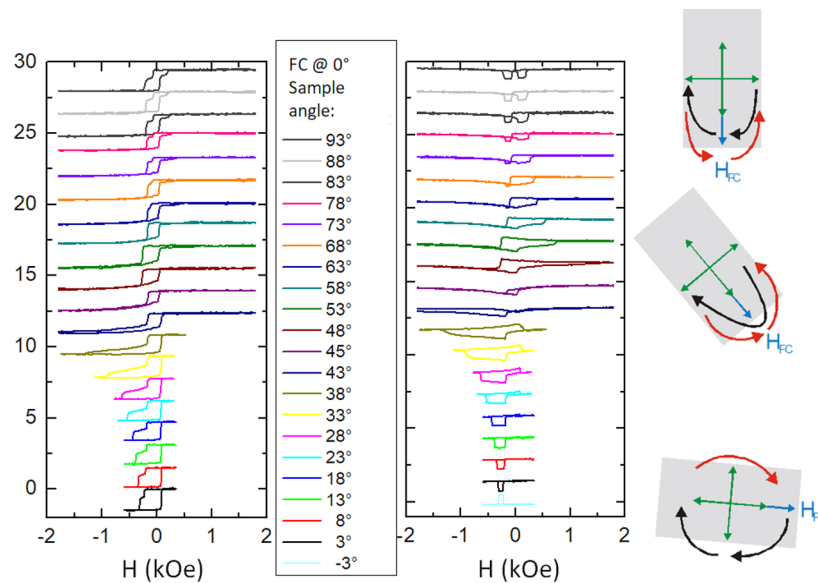


FIG. 10. Longitudinal (left) and transverse magnetization components (middle), measured after field cooling along the AFM easy axis at 0° to $T = 20$ K. Schematic representation of the magnetization reversal in different sample angle ranges. Reprinted from Tillmanns, *Magnetisierungsumkehr und -dynamik in Exchange-Bias-Systemen*, Dissertation thesis, RWTH Aachen, Germany, 2005. Copyright 2005, published open access; modified.

the range from -35° to $+35^\circ$ resulted in asymmetric magnetization reversal with rotation of the Fe magnetic moments on the left side and mostly domain wall processes on the right side, while measurements near 90° revealed magnetization reversal via the easy axis defined by the EB direction.⁵⁷ For $\text{MnF}_2(110 \text{ twinned})/\text{Fe}$ with (110) texture, very similar results were published and explained in the same way, as depicted in Fig. 10.³⁹

For a more detailed investigation of the magnetic anisotropy, Pechan *et al.* measured spin wave frequencies by ferromagnetic resonance (FMR) in an $\text{MnF}_2(110 \text{ twinned})/\text{polycrystalline Fe}$ sample and found a clearly fourfold anisotropy after field cooling to 40 K in different cooling fields, which was consistent with a cosine-shaped EB term. However, the FMR linewidths show sharp peaks in the hard directions, which could not be explained by the common model equation.⁶⁵ More detailed FMR measurements of a $\text{MnF}_2(110 \text{ twinned})/\text{polycrystalline Fe}$ sample^{66,67} and an $\text{MnF}_2(110 \text{ twinned})/\text{Fe}(110)$ sample,³⁹ compared with simulations, revealed that the common cosine term for the EB did not correctly reproduce the FMR measurements. Instead, a model was suggested including higher symmetry odd terms⁶⁷ or a simpler, but not physically deduced absolute function for the fourfold anisotropy,³⁹ which were both able to accurately fit the FMR data. In addition, Ref. 39 suggested that the EB direction could not freely vary with the cooling field direction, as in polycrystalline Fe/FeF_2 ,⁶² but should be a superposition of a partial EB along the fourfold easy axes nearest to the cooling field orientation. With these assumptions, the transverse magnetization loops depicted in Fig. 10 could well be reproduced by a macrospin model.³⁹

E. Fe/MnF_2 —Varying cooling field angles

Fe/MnF_2 samples were also investigated for varying cooling field directions. Olamit *et al.* showed that the EB in $\text{Fe}/\text{twinned MnF}_2$ samples was a nearly constant negative value in the angular range from -45° to $+45^\circ$ for FC at 0° (the easy axis), followed by an angular range around the next easy axis (45° – 135°) where the EB was negligibly small. At angles near 180° (i.e., opposite the cooling field direction), the EB again showed nearly constant positive values.⁶² Shifting the cooling field to 90° shifted the whole angular dependence of the EB also by 90° .⁶² FC at other angles was not reported, while similar results were found for $\text{Ni}/\text{twinned MnF}_2$.⁶²

Detailed measurements of the angles where the signs of the transverse peaks were switched for different cooling field orientations revealed a phase diagram quite different from those of Fe/FeF_2 [Fig. 11(a)].³⁹ These values could be simulated by a macrospin model if the EB angle was set along the easy axis that was the nearest to the cooling field direction, as shown in Fig. 11(b).³⁹ This indicates that, similar to the case of purely fourfold Fe/FeF_2 [cf. Fig. 9(b)], the EB direction in Fe/MnF_2 is approximately identical to an easy AFM axis. The difference between both samples is that the fourfold anisotropy of Fe/FeF_2 is mathematically described by a common fourfold anisotropy term, such as $[\cos^2(\phi)\sin^2(\phi)]$, while the fourfold anisotropy of Fe/MnF_2 can be much better described by a term like $|\cos(\phi)\sin(\phi)|$ with the sample angle ϕ .³⁹

It should be mentioned that similar energy landscapes with sharp peaks along the hard axes have also been found, e.g., in fourfold NiFe/FeMn double layers.⁶⁸ However, similar transverse

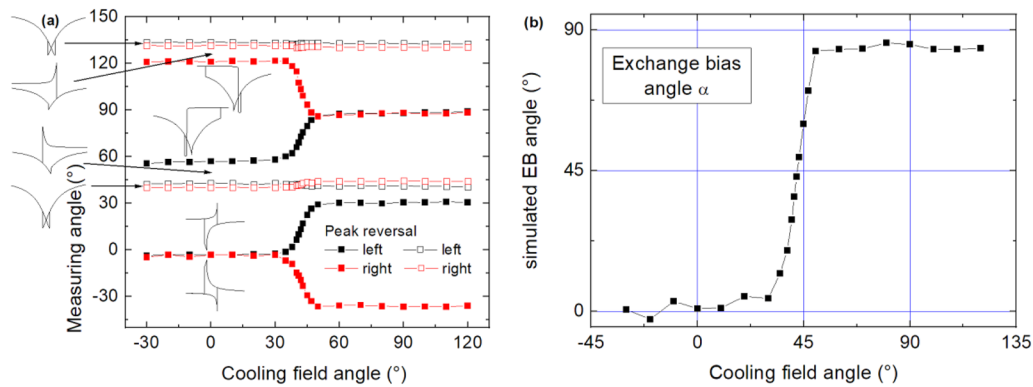


FIG. 11. (a) Measuring angles showing a peak sign change for a range of cooling field angles, measured for a Fe/MnF₂ sample. (b) EB angle vs cooling field angle, deduced from the simulation of the phase diagram. Reprinted from Tillmanns, Magnetisierungsumkehr und -dynamik in Exchange-Bias-Systemen, Dissertation thesis, RWTH Aachen, Germany, 2005. Copyright 2005, published open access; modified.

TABLE I. Overview of physical properties of Fe/FeF₂ and Fe/MnF₂.

Physical properties	Fe/FeF ₂	Fe/MnF ₂
AFM Néel temperature	78 K ²⁰	67 K ^{23,24}
Typical crystal orientation	Pseudo-twinned FeF ₂ (110); Fe spins in-plane ^{25,30,31}	Pseudo-twinned MnF ₂ (110); Fe spins in-plane ^{25–28}
Temperature-dependent T _C	Peak near T _N for untwinned (110) FeF ₂ and for twinned (110) FeF ₂ is possible ^{33,35,39}	Constantly decreasing or constant up to 75 K ^{25,41}
Temperature-dependent EB	Maximum around 30–50 K is possible ^{30,39}	Often mostly constant up to ~50 K ^{25,39,40}
Blocking temperature	Near Néel temperature ^{30,31}	Near Néel temperature ^{27,39}
Asymmetry	Asymmetric magnetization reversal for twinned FeF ₂ (110) ^{9,33,39}	Often strong asymmetry of the hysteresis loop, showing steps, and corresponding rectangular transverse signals ^{39,42,64}
Cooling-field dependence	EB can be positive for large cooling fields ^{30,43,44}	EB can be positive for large cooling fields ^{43,44}
EB dependence on in-plane angle (FC at easy axis)	Asymmetry of transverse peaks outside cooling field axis ³⁹	Asymmetry of transverse peaks outside cooling field axis; ^{57,64} FMR with sharp peaks in the hard directions ^{39,65–67} leading to higher-symmetry odd terms ⁶⁷ or absolute function ³⁹
EB dependence on in-plane angle (FC at varying angles)	Cosine-shaped EB for polycrystalline Fe/FeF ₂ ; ⁶³ EB direction can vary around the cooling field direction ⁹ or can be identical with the easy axis ³⁹ in twinned FeF ₂ (110) systems	EB direction similar to easy axis nearest to FC direction ^{39,62}

magnetization loops as in Fe/MnF₂ were also reported for other fourfold EB systems such as Fe(001)/IrMn(001).⁶⁰ This led to the assumption that the here described model can also be transferred to other EB systems.

VI. CONCLUSION AND OUTLOOK

This literature review compared the exchange-biased thin film model systems Fe/FeF₂ and Fe/MnF₂, focusing on the temperature dependence, cooling field dependence, and angular

dependence of the EB. Table I gives an overview of the varying findings.

While the EB usually shows a blocking temperature very near to the AFM's Néel temperature, in the case of Fe/FeF₂ bilayers, the temperature dependence of the coercivity is influenced by the crystallographic orientation of the iron layer. This often includes a peak of the coercivity around the Néel temperature in the case of (100) textured Fe. Depending on the cooling field, both material systems may show a positive EB. In the transverse magnetization components, Fe/MnF₂ shows broad peaks related to stable intermediate states during magnetization reversal, while Fe/FeF₂ shows narrower, more triangular-like peaks.

The angular dependence of EB and coercivity, combined with measurements at different field cooling angles, suggests that the fourfold anisotropy of Fe/FeF₂ exhibits the usual $[\cos^2(\phi)\sin^2(\phi)]$ shape, while Fe/MnF₂ is better described by a $|\cos(\phi)\sin(\phi)|$ four-fold anisotropy. While Fe/FeF₂ with a (110) textured Fe layer and a (110) twinned AFM shows smoothly varying differences between the EB direction and the cooling field orientation, the Fe/FeF₂ system with a (100) textured Fe layer and a (110) twinned AFM (as well as Fe/MnF₂) showed an EB direction parallel to an easy axis, nearly independent from the cooling field direction.

As this article demonstrates, several questions remain open, such as the influence of the Fe layer texture on Fe/MnF₂ samples, the angular dependence of EB and coercivity for samples with untwinned antiferromagnets, or the impact of the surface roughness on magnetization reversal processes. We hope that this overview stimulates more researchers to further investigate these EB systems, not only due to broadening the basic knowledge about them but also due to their potential application in spintronics devices.

Especially the combination of fourfold and unidirectional anisotropy in Fe/MnF₂ promises interesting applications in magneto-electronics, e.g., for the development of quaternary-state memories. While Fe/MnF₂ is well-suited for further basic research, future applications should be based on material systems that exhibit an EB around room temperature, such as the aforementioned Fe/IrMn,^{60,69} which have already proven to be thermally stable in magnetic tunnel junctions and other spintronic elements.⁷⁰

ACKNOWLEDGMENTS

The APC was funded by Deutsche Forschungsgemeinschaft (DFG, German Research Foundation)—490988677 and the Bielefeld University of Applied Sciences and Arts.

AUTHOR DECLARATIONS

Conflict of Interest

The authors have no conflicts to disclose.

Author Contributions

Tomasz Blachowicz: Conceptualization (equal); Methodology (equal); Writing – original draft (equal). **Maciej Malczyk:** Conceptualization (equal). **Andrea Ehrmann:** Conceptualization (equal); Methodology (equal); Validation (equal); Writing – original draft

(equal). **Martin Wortmann:** Visualization (equal); Writing – original draft (equal).

DATA AVAILABILITY

No new data were created in this review paper.

REFERENCES

- W. H. Meiklejohn and C. P. Bean, *Phys. Rev.* **102**, 1413 (1956).
- J. Nogués and I. K. Schuller, *J. Magn. Magn. Mater.* **192**, 203 (1999).
- J. Nogués, T. J. Moran, D. Lederman, I. K. Schuller, and K. V. Rao, *Phys. Rev. B* **59**, 6984 (1999).
- T. Blachowicz and A. Ehrmann, *Coatings* **11**, 122 (2021).
- J. Nogués, J. Sort, V. Langlais, V. Skumryev, S. Surinach, J. S. Muñoz, and M. D. Baró, *Phys. Rep.* **422**, 65 (2005).
- T. Blachowicz, A. Ehrmann, and M. Wortmann, *Nanomaterials* **13**, 2418 (2023).
- T. Blachowicz, A. Tillmanns, M. Fraune, B. Beschoten, G. Güntherodt, and G. Güntherodt, *Phys. Rev. B* **75**, 054425 (2007).
- M. Wortmann, T. Samanta, M. Gaerner, M. Westphal, J. Fiedler, I. Ennen, A. Hütten, T. Blachowicz, L. Caron, and A. Ehrmann, *APL Mater.* **11**, 121118 (2023).
- A. Tillmanns, S. Oertker, B. Beschoten, G. Güntherodt, J. Eisenmenger, and I. K. Schuller, *Phys. Rev. B* **78**, 012401 (2008).
- A. Tillmanns, S. Oertker, B. Beschoten, G. Güntherodt, C. Leighton, I. K. Schuller, and J. Nogués, *Appl. Phys. Lett.* **89**, 202512 (2006).
- Z. Hussain, A. K. Bera, A. S. Dev, D. Kumar, and V. R. Reddy, *J. Alloys Compd.* **849**, 156484 (2020).
- B. M. Zhang, *J. Mater. Sci. Mater. Electron.* **31**, 19875 (2020).
- A. Masood, L. Belova, and V. Ström, *J. Appl. Phys.* **134**, 243903 (2023).
- S. K. Kedia, N. Kumar, N. Sharma, and S. Chaudhary, *J. Appl. Phys.* **135**, 053903 (2024).
- C. Y. Zhang, Q. F. Zhan, Y. Hu *et al.*, *Appl. Phys. Lett.* **123**, 012404 (2023).
- C. Y. Zhang, Z. M. Zhang, D. H. Wang, and Y. Hu, *Appl. Phys. Lett.* **124**, 082407 (2024).
- S. K. Kedia, N. Sharma, L. Pandey, and S. Chaudhary, *J. Appl. Phys.* **134**, 173904 (2023).
- F. Tian, T. Chang, Q. Zhao, J. Guo, L. Xian, K. Cao, Z. Dai, Y. Zhang, C. Zhou, and S. Yang, *Appl. Phys. Lett.* **123**, 232402 (2023).
- B. C. Sales, A. L. Cabrera, and M. B. Maple, *Solid State Commun.* **30**, 119 (1979).
- M. Grimsditch, A. Hoffmann, P. Vavassori, H. T. Shi, and D. Lederman, *Phys. Rev. Lett.* **90**, 257201 (2003).
- H. Yamazaki and J. Satooka, *J. Magn. Magn. Mater.* **240**, 442 (2002).
- J. X. Li, Z. Shi, V. H. Ortiz, M. Aldosary, C. Chen, V. Aji, P. Wei, and J. Shi, *Phys. Rev. Lett.* **122**, 217204 (2019).
- P. Heller, *Phys. Rev.* **146**, 403 (1966).
- J. C. Burgiel and M. W. P. Strandberg, *J. Phys. Chem. Solids* **26**, 865 (1965).
- B. Sahoo, "Spin structure of exchange biased heterostructures: Fe/MnF₂ and Fe/FeF₂," Dissertation thesis, Universität Duisburg-Essen, Germany, 2006.
- W. Keune, *Hyperfine Interact.* **204**, 13 (2012).
- M. R. Fitzsimmons, C. Leighton, A. Hoffmann, P. C. Yashar, J. Nogués, K. Liu, C. F. Majkrzak, J. A. Dura, H. Fritzsche, and I. K. Schuller, *Phys. Rev. B* **64**, 104415 (2001).
- W. A. A. Macedo, B. Sahoo, J. Eisenmenger, M. D. Martins, W. Keune, V. Kuncser, R. Röhlberger, O. Leupold, R. Rüffer, J. Nogués, K. Liu, K. Schlage, and I. K. Schuller, *Phys. Rev. B* **78**, 224401 (2008).
- M. L. Silva, A. L. Dantas, and A. S. Carrico, *J. Magn. Magn. Mater.* **292**, 453 (2005).
- J. Nogués, D. Lederman, T. J. Moran, and I. K. Schuller, *Phys. Rev. Lett.* **76**, 4624 (1996).
- J. Nogués, T. J. Moran, D. Lederman, I. K. Schuller, and K. V. Rao, *Phys. Rev. B* **59**, 6984 (1999).
- M. Kiwi, J. Mejía-López, R. D. Portugal, and R. Ramirez, *Europhys. Lett.* **48**, 573 (1999).

- ³³M. R. Fitzsimmons, C. Leighton, J. Nogués, A. Hoffmann, K. Liu, C. F. Majkrzak, J. A. Dura, J. R. Groves, R. W. Springer, P. N. Arendt, V. Leiner, H. Lauter, and I. K. Schuller, *Phys. Rev. B* **65**, 134436 (2002).
- ³⁴M. R. Fitzsimmons, P. Yashar, C. Leighton, I. K. Schuller, J. Nogués, C. F. Majkrzak, and J. A. Dura, *Phys. Rev. Lett.* **84**, 3986 (2000).
- ³⁵T. J. Moran, J. Nogués, D. Lederman, and I. K. Schuller, *Appl. Phys. Lett.* **72**, 617 (1998).
- ³⁶S. Widuch, Z. Celinski, K. Balin, R. Schäfer, L. Schultz, D. Skrzypek, and J. McCord, *Phys. Rev. B* **77**, 184433 (2008).
- ³⁷U. Nowak, K. D. Usadel, J. Keller, P. Miltényi, B. Beschoten, and G. Güntherodt, *Phys. Rev. B* **66**, 014430 (2002).
- ³⁸Y. Li, J.-H. Moon, and K.-J. Lee, *J. Magn.* **16**, 323 (2011).
- ³⁹A. Tillmanns, “Magnetisierungsumkehr und -dynamik in Exchange-Bias-Systemen,” Dissertation thesis, RWTH Aachen, Germany, 2005.
- ⁴⁰W. A. A. Macedo, B. Sahoo, V. Kuncser, J. Eisenmenger, I. Felner, J. Nogués, K. Liu, W. Keune, and I. K. Schuller, *Phys. Rev. B* **70**, 224414 (2004).
- ⁴¹C. Leighton, M. R. Fitzsimmons, A. Hoffmann, J. Dura, C. F. Majkrzak, M. S. Lund, and I. K. Schuller, *Phys. Rev. B* **65**, 064403 (2002).
- ⁴²C. Leighton, M. R. Fitzsimmons, P. Yashar, A. Hoffmann, J. Nogués, J. Dura, C. F. Majkrzak, and I. K. Schuller, *Phys. Rev. Lett.* **86**, 4394 (2001).
- ⁴³J. Nogués, C. Leighton, and I. K. Schuller, *Phys. Rev. B* **61**, 1315 (2000).
- ⁴⁴M. Kiwi, J. Mejía-López, R. D. Portugal, and R. Ramírez, *Solid State Commun.* **116**, 315 (2000).
- ⁴⁵L. Sun and H. Xing, *J. Appl. Phys.* **104**, 043904 (2008).
- ⁴⁶J. Geshev, S. Nicolodi, L. G. Pereira, L. C. C. M. Nagamine, J. E. Schmidt, C. Deranlot, F. Petroff, R. L. Rodríguez-Suárez, and A. Azevedo, *Phys. Rev. B* **75**, 214402 (2007).
- ⁴⁷E. Jiménez, J. Camarero, J. Sort, J. Nogués, N. Mikuszeit, J. M. García-Martín, A. Hoffmann, B. Dieny, and R. Miranda, *Phys. Rev. B* **80**, 014415 (2009).
- ⁴⁸H. T. Shi, “Exchange bias and its angular dependence in $\text{Fe}_x\text{Zn}_{1-x}\text{F}_2/\text{Co}$ bilayers,” Dissertation thesis, West Virginia University, 2002.
- ⁴⁹J. Tang, B. F. P. Roos, T. Mewes, A. R. Frank, M. Rickart, M. Bauer, S. O. Demokritov, B. Hillebrands, X. Zhou, B. Q. Liang, X. Chen, and W. S. Zhan, *Phys. Rev. B* **62**, 8654 (2000).
- ⁵⁰C. Binek, A. Hochstrat, and W. Kleemann, *J. Magn. Magn. Mater.* **234**, 353–358 (2001).
- ⁵¹E. Cardelli, A. Faba, G. Finocchio, and B. Azzarboni, *IEEE Trans. Magn.* **48**, 3367–3370 (2012).
- ⁵²F. Radu, A. Westphalen, K. Theis-Bröhl, and H. Zabel, *J. Phys.: Condens. Matter* **18**, L29 (2006).
- ⁵³J. Geshev, L. G. Pereira, and J. E. Schmidt, *Phys. Rev. B* **66**, 134432 (2002).
- ⁵⁴B. B. Singh and S. Chaudhary, *J. Magn. Magn. Mater.* **385**, 166 (2015).
- ⁵⁵S. Dubourg, J. F. Bobo, B. Warot, E. Snoeck, and J. C. Ousset, *Eur. Phys. J. B* **45**, 175 (2005).
- ⁵⁶A. Ehrmann and T. Blachowicz, *J. Appl. Phys.* **109**, 083923 (2011).
- ⁵⁷M. O. Liedke, B. Liedke, A. Keller, B. Hillebrands, A. Mücklich, S. Fasco, and J. Fassbender, *Phys. Rev. B* **75**, 220407(R) (2007).
- ⁵⁸K. Gandha, R. P. Chaudhary, J. Mohapatra, A. R. Kymen, and J. P. Liu, *Phys. Lett. A* **381**, 2092–2096 (2017).
- ⁵⁹F. Radu, S. K. Mishra, I. Zizak, A. I. Erko, H. A. Dürr, W. Eberhardt, G. Nowak, S. Buschhorn, K. Zhernenkov, M. Wolff, H. Zabel, D. Schmitz, E. Schierle, E. Dudzik, and R. Feyerherm, *Phys. Rev. B* **79**, 184425 (2009).
- ⁶⁰W. Zhang and K. M. Krishnan, *J. Magn. Magn. Mater.* **324**, 3129 (2012).
- ⁶¹T. Hajiri, T. Yoshida, S. Jaiswal, M. Filianina, B. Borie, H. Ando, H. Asano, H. Zabel, and M. Kläui, *Phys. Rev. B* **94**, 184412 (2016).
- ⁶²P. Miltényi, M. Gruyters, G. Güntherodt, J. Nogués, and I. K. Schuller, *Phys. Rev. B* **59**, 3333 (1999).
- ⁶³J. Olamit, Z.-P. Li, I. K. Schuller, and K. Liu, *Phys. Rev. B* **73**, 024413 (2006).
- ⁶⁴E. Arenholz and K. Liu, *Appl. Phys. Lett.* **87**, 132501 (2005).
- ⁶⁵M. J. Pechan, D. Bennett, N. C. Teng, C. Leighton, J. Nogués, and I. K. Schuller, *Phys. Rev. B* **65**, 064410 (2002).
- ⁶⁶I. N. Krivorotov, C. Leighton, J. Nogués, I. K. Schuller, and E. D. Dahlberg, *Phys. Rev. B* **65**, 100402(R) (2002).
- ⁶⁷I. N. Krivorotov, C. Leighton, J. Nogués, I. K. Schuller, and E. D. Dahlberg, *Phys. Rev. B* **68**, 054430 (2003).
- ⁶⁸T. Mewes, B. Hillebrands, and R. L. Stamps, *Phys. Rev. B* **68**, 184418 (2003).
- ⁶⁹W. Zhang, M. E. Bowden, and K. M. Krishnan, *Appl. Phys. Lett.* **98**, 092503 (2011).
- ⁷⁰M. G. Samant, J. Lüning, J. Stöhr, and S. S. P. Parkin, *Appl. Phys. Lett.* **76**, 3097 (2000).